

Regularizing kernel-based BRDF model inversion method for ill-posed land surface parameter retrieval using smoothness constraint

Yanfei Wang,¹ Changchun Yang,¹ and Xiaowen Li²

Received 23 August 2007; revised 17 January 2008; accepted 19 February 2008; published 1 July 2008.

[1] In this paper, we consider the problem how to solve the kernel-based bidirectional reflectance distribution function (BRDF) models for the retrieval of land surface albedos. The above problem is an ill-posed inverse problem. We will employ a new regularization technique to alleviate the ill-posedness. The Tikhonov regularization has been discussed for BRDF model inversion, however, much study has to be done before applying it in practice (Wang et al., 2007). In this paper, we thoroughly investigate this method, and propose a discrepancy method for a posteriori choice of the regularization parameter and several options for choosing the regularizing stabilizer. The proposed method can alleviate difficulties in numerical computation when the discrete kernel is badly conditioned and the number of observations is poor. Applying the proposed method can always find a set of suitable BRDF coefficients for poorly sampled data. The proposed method is an improvement of the traditional least squares error algorithm in AMBRALS (Algorithm for MODIS (Moderate Resolution Imaging Spectroradiometer) Bidirectional Reflectance Anisotropies of the Land Surface), see Strahler et al. (1999), and is comparable to the regularized singular value decomposition method developed by Wang et al. (2007). Hence the proposed method can be considered as a supplemental algorithm for the robust estimation of the land surface BRDF/albedos. Numerical performance is given in this paper for the widely used field-based 18 data sets among the 73 data sets (see Li et al., 2001) and for the satellite data.

Citation: Wang, Y., C. Yang, and X. Li (2008), Regularizing kernel-based BRDF model inversion method for ill-posed land surface parameter retrieval using smoothness constraint, *J. Geophys. Res.*, 113, D13101, doi:10.1029/2007JD009324.

1. Introduction

[2] It is well-known that the anisotropy of the land surface can be described by the bidirectional reflectance distribution function (BRDF). It is known that the BRDF models can be inverted to estimate the important biological or climatological parameters of the Earth surface, such as leaf area index and albedo [see Strahler et al., 1994]. The information extraction on the terrestrial biosphere and other problems for retrieval of land surface albedos from satellite remote sensing have been considered by many authors in recent years, see for instance the survey papers on the kernel-based bidirectional reflectance distribution function (BRDF) models by Pokrovsky and Roujean [2002, 2003]; Pokrovsky et al. [2003]. The state-of-the-art BRDF is to use the linear kernel-based models, which can be mathematically described as the linear combination of the isotropic kernel, volume scattering kernel, and geometric optics

kernel. The retrieval of the model coefficients is of great importance for determining the land surface albedos. Other than observation errors a limited or insufficient number of observations is one of the most severe obstacles for the estimation of BRDF. Therefore it is very desirable to develop new techniques for the robust estimation of the BRDF model parameters due to the scarcity of the number of observations. In the work of Pokrovsky and Roujean [2002], the authors utilized the *QR* decomposition and also suggested using the singular value decomposition for the inversion of the BRDF model. Later by Pokrovsky et al. [2003], they compared several inversion techniques and uncertainty in albedo estimates from the SEVIRI/MSG observing system by using POLDER BRDF measurements. The method by Pokrovsky et al. [2003] is quite statistical, which does not require the selection of regularization parameter, and hence it has high accuracy. But on the other hand, that method requires some a priori information on class of solution in search. In a study by Wang et al. [2005], the authors proposed an interior point solution method for the retrieval of land surface parameters, which utilizes the least norm as an a priori, and obtain some stable numerical results. In the studies of Wang et al. [2006b, 2007], the authors performed successive tests to verify the feasibility of the singular value decomposition method and proposed a

¹Institute of Geology and Geophysics, Chinese Academy of Sciences, Beijing, China.

²State Key Laboratory of Remote Sensing Science and Research Center for Remote Sensing and GIS, Beijing Normal University, Beijing, China.

regularized version of the singular value decomposition method.

[3] The linear kernel-based BRDF model can be described as follows [see *Roujean et al.*, 1992]:

$$f_{iso} + k_{vol}(t_i, t_v, \phi)f_{vol} + k_{geo}(t_i, t_v, \phi)f_{geo} = r(t_i, t_v, \phi), \quad (1)$$

where r is the bidirectional reflectance; the kernels k_{vol} and k_{geo} are so-called kernels, that is, known functions of illumination and of viewing geometry which describe volume and geometric scattering respectively; t_i and t_v are the zenith angle of the solar direction and the zenith angle of the view direction respectively; ϕ is the relative azimuth of sun and view direction; and f_{iso} , f_{vol} and f_{geo} are three unknown parameters to be adjusted to fit observations. Theoretically, f_{iso} , f_{vol} and f_{geo} are closely related to the biomass such as leaf area index (LAI), Lambertian reflectance, sunlit crown reflectance, and viewing and solar angles. The vital task then is to retrieve appropriate values of the three parameters.

[4] Generally speaking, the BRDF model includes kernels of many types. However, it was demonstrated that the combination of RossThick (k_{vol}) and LiSparse (k_{geo}) kernels had the best overall ability to fit BRDF measurements and to extrapolate BRDF and albedo [see *Hu et al.*, 1997; *Wanner et al.*, 1995; *Li et al.*, 1999; *Privette et al.*, 1997]. A suitable expression for the RossThick kernel k_{vol} was derived by *Roujean et al.* [1992]. In this paper we will use the LiTransit kernel $k_{Transit}$ instead of the kernel k_{geo} since it is more robust and stable than LiSparse nonreciprocal kernel and the reciprocal LiSparse kernel k_{sparse} (LiSparseR) where the LiTransit kernel and the LiSparse kernel are related by

$$k_{Transit} = \begin{cases} k_{sparse}, & B \leq 2, \\ \frac{2}{B}k_{sparse}, & B > 2, \end{cases} \quad (2)$$

and B is given

$$B := B(t_i, t_v, \phi) = -O(t_i, t_v, \phi) + \text{sect}'_i + \text{sect}'_v$$

by *Li et al.* [2000]. More detailed explanation about O and t' in the definition of $k_{Transit}$ are discussed by *Wanner et al.* [1995]. We will use the combination of RossThick kernel and LiTransit kernel in the numerical tests.

[5] To use the combined linear kernel model, a key issue is to numerically solve the inverse model in a stable way. However, it is difficult to do in practical applications due to ill-posed nature of the inverse problem. It is suggested by *Wang et al.* [2007], to fully employ the regularization theory to tackle the difficulty. In this paper, we will investigate the method by imposing smoothness constraint and develop an *a posteriori* technique for choosing the regularization parameter.

[6] This paper is organized as follows: in section 2, we study the regularization methods in great detail for solving the BRDF model. We discuss the ill-posed nature of the problem in section 2.1; propose some smooth constraints for regularization in section 2.2; present the variational regularization in section 2.3; discuss the problem how to select the smooth operator in sections 2.4 and 2.5; and

address an *a posteriori* choice of the regularization parameter in section 2.6. Section 3 is devoted to several numerical simulations to demonstrate our algorithm. In section 4, some concluding remarks are given. Finally, we provide appendices for deducing the *a posteriori* technique for choosing the regularization parameter, for differentiation of the Tikhonov functional, and for an appendix for subroutine instructions on implementing the algorithm proposed in this paper.

[7] Throughout the paper, we use the following notations: “:=” denotes “defined as”; “min” denotes “minimizing” some functional; \mathbf{x} and x denote the vector and the continuous function respectively, so to other functions and their corresponding vectors; “ K^* ” denote the adjoint of an operator K ; “ K^T ” denote the transpose of matrix K , and $\text{diag}(\cdot)$ denotes a diagonal matrix.

2. Regularization for Parameter Retrieval by Imposing Smoothness Constraint

[8] The BRDF model (1), a linear kernel-based model, can be formulated as the following finite rank operator equation

$$K\mathbf{x} = \mathbf{y}, \quad (3)$$

where $K \in \mathbb{R}^{M \times N}$ is the coefficient matrix, $\mathbf{x} \in \mathbb{R}^N$ is the parameter to be retrieved, and $\mathbf{y} \in \mathbb{R}^M$ is the measurement. The inversion of finite rank operator equations is discrete ill-posed in general, it is of great importance how to find a suitable method to stably retrieve the BRDF model parameters. To tackle this difficulty, we intend to apply the regularization theory and related methods to the BRDF model parameter retrieval problem.

2.1. Ill-Posedness

[9] The ill-posedness arises because the linear kernel-based BRDF model is underdetermined, for instance when there are too few observations or poor directional range. A single angular observation may lead to an underdetermined system whose solution set is infinite (the null-space of the operator contains nonzero vectors) or no solution (the rank of the coefficient matrix is not equal to the rank of the augmented matrix). Another reason that leads to the ill-posedness is that error/noise propagation is significantly enlarged in computation due to bad algebraic spectrum distribution [see, e.g., *Wang et al.*, 2007]. Because of the ill-posedness of the inversion process, uncertainties in the model and in the reflectance measurements do not simply result in uncertainties on the solution. More severely, the ill-posedness may lead to jumps in the solution space, i.e., the solution found may spread in the whole parameter space instead of being centered on the true solution [see *Xiao et al.*, 2003; *Atzberger*, 2004; *Tikhonov and Arsenin*, 1977; *Wang*, 2007]. To alleviate those difficulties, it is necessary to impose *a priori* information [see, e.g., *Tarantola*, 1987]. As is noted by *Wang et al.* [2007], different kinds of *a priori* information can be employed. We adopt a popular *a priori* information that simplifies the physical model by solving a l_p ($p = 2$) norm problem, which means the unknowns \mathbf{x} can be obtained under the l_p scale.

2.2. Smoothness Constraint

[10] The incorporation of a priori constraints may lead to the stabilization of the ill-posed problem. However, the incorporation of constraints is not a trivial task, which may come from several sources, historically, empirically or quantitatively. For land surface parameter retrieval problems, quantitative nature can be imposed to the entire set of parameters. This information can be easily incorporated into the mathematical functionals. More specifically, we presents in the next subsection a mathematical functional that incorporates the notion of smoothness of the land surface parameters. In other words, the variation of the parameters in the physical process is smooth. Hence regularization can be realized by knowing that the parameter distribution varies smoothly. We will show that, by the appropriate selection of this kind of constraints in the objective functional to be minimized, both the uncertainty in the estimates of the inverted parameters can be reduced and the accuracy toward more realistic estimates can be obtained. In other words, by incorporating appropriate constraints, we are able to fit the observation data well and to estimate representative parameters of the land surfaces.

2.3. Variational Regularization

[11] Most of inverse problems in real environment are generally ill-posed. Regularization methods are widely used to solve such ill-posed problems. The complete theory for regularization was developed by Tikhonov and his colleagues [see *Tikhonov and Arsenin, 1977*]. For the discrete model (3), we suppose \mathbf{y} is the true right-hand side, and denote \mathbf{y}_n the measurements with noise which represents the bidirectional reflectance. The Tikhonov regularization method is to solve a regularized minimization problem

$$J^\alpha(\mathbf{x}) := \|K\mathbf{x} - \mathbf{y}_n\|_2^2 + \alpha \|D^{1/2}\mathbf{x}\|_2^2 \rightarrow \min \quad (4)$$

instead of solving

$$J(\mathbf{x}) = \|K\mathbf{x} - \mathbf{y}_n\|_2^2 \rightarrow \min. \quad (5)$$

In (4), α is the regularization parameter and D is a positively (semi)definite operator. By a variational process (see Appendix B), the minimizer of (4) satisfies

$$K^T K\mathbf{x} + \alpha D\mathbf{x} = K^T \mathbf{y}_n. \quad (6)$$

The operator D is a scale matrix which imposes smoothness constraint to the solution \mathbf{x} . Apparently, the solution can be written as

$$\mathbf{x} = (K^T K + \alpha D)^{-1} K^T \mathbf{y}_n. \quad (7)$$

The scale operator D and the regularization parameter α can be considered as some kind of a priori information, which will be discussed next.

2.4. Choice of the Scale Operator D

[12] To regularize the ill-posed problem discussed in the previous subsection, the choice of the scale operator D has great impact to the performance to the regularization. Note that the matrix D plays the role in imposing a smoothness

constraint to the parameters and in improving the condition of the spectrum of the adjoint operator $K^T K$. Therefore it should be positively definite or at least positively semi-definite. One may readily see that the identity may be a choice. However, this choice does not fully employ the assumption about the continuity of the parameters.

[13] In the work of *Wang et al. [2007]*, we assume that the operator equation (3) is the discretized version of a continuous physical model

$$K(x(\tau)) = y(\tau) \quad (8)$$

with K the linear/nonlinear operator, $x(\tau)$ the complete parameters describing the land surfaces and y the observation. Most of the kernel model methods reported in literature may have the above formulation. Hence instead of establishing regularization for the operator equation (3) in the Euclidean space, it is more convenient to perform the regularization to the operator equation (8) on an abstract space. So from a priori considerations we suppose that the parameters x is a smooth function, in the sense that x is continuous on $[a, b]$, is differentiable almost everywhere and its derivative is squareintegrable on $[a, b]$. By Sobolev's imbedding theorem [see, e.g., *Tikhonov and Arsenin, 1977; Xiao et al., 2003*], the continuous differentiable function x in $W^{1,2}$ space imbeds into integrable continuous function space L_2 automatically. Here, the L_2 space is defined as the set of functions which are square-integrable, i.e., $L_2(\Omega) := \{x(t): \int_\Omega |x(t)|^2 dt < \infty\}$; the Sobolev $W^{1,2}$ space is defined as the set of functions which are continuous and differentiable with the bounded norms of itself and its generalized derivatives in L_2 , i.e., $W^{1,2}(\Omega) := \{x(t): x(t) \in C(\Omega), x(t) \in L_2(\Omega), \frac{dx}{dt} \in L_2(\Omega), \int_\Omega (x^2 + \sum_{i=1}^n (\frac{dx}{dt_i})^2) dt_1 dt_2 \cdots dt_n < \infty\}$, where $C(\Omega)$ denotes the continuous space. The inner product of two functions $x(\tau)$ and $y(\tau)$ in $W^{1,2}$ space is defined by

$$(x(\tau), y(\tau))_{W^{1,2}} := \int_\Omega \left(x(\tau)y(\tau) + \sum_{i=1}^n \frac{\partial x}{\partial \tau_i} \frac{\partial y}{\partial \tau_i} \right) d\tau_1 d\tau_2 \cdots d\tau_n, \quad (9)$$

where Ω is the assigned interval of the definition.

[14] Now we construct a regularizing algorithm that an approximate solution $x^\alpha \in W^{1,2}[a, b]$ which converges, as error level approaching zero, to the actual parameters in the norm of space $W^{1,2}[a, b]$, precisely we construct the functional

$$J^\alpha[x] = \rho_F[Kx, y] + \alpha L(x), \quad (10)$$

where

$$\rho_F[Kx, y] = \frac{1}{2} \|Kx - y\|_{L_2}^2$$

and

$$L(x) = \frac{1}{2} \|x\|_{W^{1,2}}^2.$$

[15] Assume that the variation of $x(\tau)$ is flat near the boundary of the integral interval $[a, b]$. In this case, the derivatives of x are zeros at the boundary of $[a, b]$. Let h_r be the step size of the grids in $[a, b]$, which could be equidistant or adaptive. Then after discretization of $L(x)$, D is a tri-diagonal matrix in the form

$$D := D_1 = \begin{bmatrix} 1 + \frac{1}{h_r^2} & -\frac{1}{h_r^2} & 0 & \cdots & 0 \\ -\frac{1}{h_r^2} & 1 + \frac{2}{h_r^2} & -\frac{1}{h_r^2} & \cdots & 0 \\ \vdots & \ddots & \ddots & \ddots & \vdots \\ 0 & \cdots & -\frac{1}{h_r^2} & 1 + \frac{2}{h_r^2} & -\frac{1}{h_r^2} \\ 0 & \cdots & 0 & -\frac{1}{h_r^2} & 1 + \frac{1}{h_r^2} \end{bmatrix}.$$

For the linear model (1), after the kernel normalization, we may consider $[a, b] = [-1, 1]$. Thus D is in the above form with $h_r = 2/(N-1)$.

2.5. Remarks on Choosing a Scale Operator D

[16] There are many kinds of techniques for choosing the scale matrix D appropriately. In Phillips-Twomey's formulation of regularization [see, e.g., Wang et al., 2006a], the matrix D is created by the norm of the second differences, $\sum_{i=2}^{N-1} (x_{i-1} - 2x_i + x_{i+1})^2$, which leads to the following form of matrix D

$$D := D_2 = \begin{bmatrix} 1 & -2 & 1 & 0 & 0 & 0 & \cdots & 0 & 0 & 0 & 0 \\ -2 & 5 & -4 & 1 & 0 & 0 & \cdots & 0 & 0 & 0 & 0 \\ 1 & -4 & 6 & -4 & 1 & 0 & \cdots & 0 & 0 & 0 & 0 \\ 0 & 1 & -4 & 6 & -4 & 1 & \cdots & 0 & 0 & 0 & 0 \\ \vdots & \vdots & \ddots & \ddots & \ddots & \ddots & \ddots & \vdots & \vdots & \vdots & \vdots \\ 0 & 0 & 0 & \cdots & 0 & 1 & -4 & 6 & -4 & 1 & 0 \\ 0 & 0 & 0 & \cdots & 0 & 0 & 1 & -4 & 6 & -4 & 1 \\ 0 & 0 & 0 & \cdots & 0 & 0 & 0 & 1 & -4 & 5 & -2 \\ 0 & 0 & 0 & \cdots & 0 & 0 & 0 & 0 & 1 & -2 & 1 \end{bmatrix}.$$

However, the matrix D is badly conditioned and thus the solution to minimize the functional $J^\alpha[x]$ with D as the smooth constraint is observed to have some oscillations [Wang et al., 2006a, 2006b]. Another option is the negative Laplacian [see e.g., Wang and Yuan, 2003; Wang, 2007]:

$$Lx := - \sum_{i=1}^n \frac{\partial^2 x}{\partial \tau_i^2}, \quad (11)$$

for which the scale matrix D for the discrete form of the negative Laplacian Lx is

$$D := D_3 = \begin{bmatrix} 1 & -1 & 0 & \cdots & 0 & 0 \\ -1 & 2 & -1 & \cdots & 0 & 0 \\ \vdots & \vdots & \vdots & \cdots & \ddots & \ddots \\ 0 & 0 & 0 & -1 & 2 & -1 \\ 0 & 0 & 0 & \cdots & -1 & 1 \end{bmatrix}.$$

Where we assume that the discretization step length as 1. The scale matrix D_3 is positive semidefinite but not positive definite and hence the minimization problem may not work efficiently for severely ill-posed inverse problems. Another option of the scale matrix D is the identity, i.e., $D = D_4 = \text{diag}(e)$, where e is the components of all ones, however this scale matrix is too conservative and may lead to over-regularization.

2.6. A Posteriori Parameter Selection Method

[17] As noted above, the choice of the regularization parameter α is important to tackle the ill-posedness. A priori choice of the parameter α allows $0 < \alpha < 1$. However, the a priori choice of the parameter does not reflect the degree of approximation that may lead to either over-estimate or under-estimate of the regularizer.

[18] We will use the widely used discrepancy principle [see Tikhonov and Arsenin, 1977; Tikhonov et al., 1995; Xiao et al., 2003] to find an optimal regularization parameter. In fact, the optimal parameter α^* is a root of the nonlinear function

$$\Psi(\alpha) = \|K\mathbf{x}_\alpha - \mathbf{y}_n\|^2 - \delta^2, \quad (12)$$

where δ is the error level to specify the approximate degree of the observation to the true noiseless data. Noting $\Psi(\alpha)$ is differentiable, fast algorithms for solving the optimal parameter α^* can be implemented. In this paper we will use the cubic convergent algorithm developed by Wang and Xiao [2001]:

$$\alpha_{k+1} = \alpha_k - \frac{2\Psi(\alpha_k)}{\Psi'(\alpha_k) + \left(\Psi'(\alpha_k)^2 - 2\Psi(\alpha_k)\Psi''(\alpha_k)\right)^{\frac{1}{2}}}. \quad (13)$$

In the above cubic convergent algorithm, the function $\Psi'(\alpha)$ and $\Psi(\alpha)$ have the following explicit expression:

$$\Psi'(\alpha) = -\alpha\beta'(\alpha),$$

$$\Psi''(\alpha) = -\beta'(\alpha) - 2\alpha \left[\left\| \frac{d\mathbf{x}_\alpha}{d\alpha} \right\|_2 + \left(\mathbf{x}_\alpha, \frac{d^2\mathbf{x}_\alpha}{d\alpha^2} \right) \right],$$

where $\beta(\alpha) = \|\mathbf{x}_\alpha\|_2^2$, $\beta'(\alpha) = 2\left(\frac{d\mathbf{x}_\alpha}{d\alpha}, \mathbf{x}_\alpha\right)$, and \mathbf{x}_α , $\frac{d\mathbf{x}_\alpha}{d\alpha}$ and $\frac{d^2\mathbf{x}_\alpha}{d\alpha^2}$ can be obtained by solving the following equations:

$$(K^T K + \alpha D)\mathbf{x}_\alpha = K^T \mathbf{y}_n, \quad (14)$$

$$(K^T K + \alpha D) \frac{d\mathbf{x}_\alpha}{d\alpha} = -D\mathbf{x}_\alpha, \quad (15)$$

$$(K^T K + \alpha D) \frac{d^2\mathbf{x}_\alpha}{d\alpha^2} = -2D \frac{d\mathbf{x}_\alpha}{d\alpha}. \quad (16)$$

[19] To solve the linear matrix-vector equations (14)–(16), we use the Cholesky (square root) decomposition method. A remarkable characteristic of the solution of

(14)–(16) is that the Cholesky decomposition of the coefficient matrix $K^TK + \alpha D$ needs only once, then the three vectors \mathbf{x}_α , $d\mathbf{x}_\alpha/d\alpha$, $d^2\mathbf{x}_\alpha/d\alpha^2$ can be obtained cheaply. Detailed description on implementing the algorithm is given in Appendix C.

3. Numerical Performance

3.1. Preliminaries

[20] Denote by M the number of measurements in the kernel-based models. Then the operator equation (3) can be rewritten in the following matrix-vector form

$$K\mathbf{x} = \mathbf{y}, \quad (17)$$

where

$$K = \begin{bmatrix} 1 & k_{geo}(1) & k_{vol}(1) \\ 1 & k_{geo}(2) & k_{vol}(2) \\ \vdots & \vdots & \vdots \\ 1 & k_{geo}(M) & k_{vol}(M) \end{bmatrix},$$

$$\mathbf{x} = \begin{bmatrix} f_{iso} \\ f_{geo} \\ f_{vol} \end{bmatrix}, \quad \mathbf{y} = \begin{bmatrix} r_1 \\ r_2 \\ \vdots \\ r_M \end{bmatrix}.$$

In practice, the coefficient matrix K cannot be determined accurately, and a perturbed version \tilde{K} is obtained instead. Also instead of the true measurement \mathbf{y} , the observed measurement $\mathbf{y}_n = \mathbf{y} + \mathbf{n}$ is the addition of the true measurement \mathbf{y} and the noise \mathbf{n} , which for simplicity is assumed to be additive Gaussian random noise. Therefore it suffices to solve the following operator equation with perturbation

$$\tilde{K}\mathbf{x} = \mathbf{y}_n.$$

Where $\tilde{K} = K + \delta B$ for some perturbation matrix B and δ denotes the noise level (upper bound) of \mathbf{n} in $(0, 1)$. In our numerical simulation, we assume that B is a Gaussian random matrix, and also that

$$\|\mathbf{y}_n - \mathbf{y}\| \leq \delta < \|\mathbf{y}_n\|. \quad (18)$$

The above assumption about the noise can be interpreted as that the signal-to-noise ratio (SNR) should be greater than 1. We make such an assumption as we believe that observations (BRDF) are not trustable otherwise. It is clear that (17) is an underdetermined system if $M \leq 2$ and an overdetermined system if $M > 3$. Note that for satellite remote sensing, because of the restrictions in view and illumination geometries, $\tilde{K}^T\tilde{K}$ needs not have bounded inverse [see *Gao et al.*, 1998; *Verstraete et al.*, 1996; *Li et al.*, 2001]. We believe that the proposed regularization method can be employed to find an approximate solution $\mathbf{x}_\alpha^\dagger$ satisfies

$$\|\tilde{K}\mathbf{x}_\alpha^\dagger - \mathbf{y}_n\| \rightarrow \min.$$

Table 1. Data Sets Used in the Simulation

Data	Cover Type	LAI
Ranson_soy.827	soy	2.9
Kimes.orchgrass	orchard grass	1
Parabola.1994.asp-ifc2	aspen	5.5

[21] In the following, we demonstrate several numerical tests for computing the land surface parameters by using the field observed data in Table 1 and the moderate resolution imaging spectroradiometer (MODIS) satellite data and Landsat TM data. To demonstrate the feasibility of our algorithm, we first apply our proposed regularization method to ill-posed field-observed data. Then, we apply it to the satellite data, where only one observation is provided.

3.2. Tests on Ill-Posed Field-Observed Data

[22] In this test, we choose the widely used 73 data sets referred by *Li et al.* [2001]. Among the 73 sets of BRDF measurements, only 18 sets of field-measured BRDF data with detailed information about the experiments are known, including biophysical and instrumental information [see *Hu et al.*, 1997; *Deering et al.*, 1992, 1994, 1995; *Eck and Deering*, 1992; *Kimes et al.*, 1985, 1986]. These data sets cover a large variety of vegetative cover types, and are fairly well representative of the natural and cultivated vegetation. Table 1 summarizes the basic properties of the data sets used in this paper. For those selected field data, the observations are sufficient. If the kernel matrix \tilde{K} is well-conditioned, the problem is well-posed, and the regularization is unnecessary, which can also be considered a regularization procedure with zero regularization parameter. Even for sufficient observations, most of the kernel matrix \tilde{K} could be ill-conditioned, and hence the problem is discrete ill-posed. In that situation, one has to resort to regularization or preconditioning to make the proposed algorithm workable. Our proposed method is quite adaptive no matter whether the kernel matrix \tilde{K} is ill-conditioned or well-conditioned.

[23] With the nice field data, the numerical experiment can be done to test the robustness of the algorithm by using a limited number of observations, and then to compare the retrieval with the measurements. The ill-posed situations are generated by significantly reducing the number of observations from the field data in Table 1.

[24] We choose one or two observations as limited number of observations and compare the retrieval results by our proposed regularization methods with the regularized singular value decomposition (NTSVD) [see *Wang et al.*, 2007]. Comparison results are given in Tables 2 and 3. We do not list all of the results since the data sets can be used to generate an enormous number of such kinds of ill-posed situations. In the two tables, these methods are denoted by NTSVD, Tikh(a) ($\alpha = \delta^2$), Tikh(b) (D is in the form of D_1 and α is chosen by a posteriori method addressed in section 2.6), Tikh(c) (D is in the form D_2 and α is chosen by a posteriori method addressed in section 2.6), Tikh(d) (D is in the form D_3 and α is chosen by a posteriori method addressed in section 2.6), and Tikh(e) (D is in the form D_4 and α is

Table 2. Comparison of Computational Values of the WSAs From Data Sets in Table 1 for Single Observation and for Two Observations With the True WSAs Values (Multiangular Observations) for VisRed Band

	Methods	Single Observation	Two Observations	True WSAs
Ranson_soy.827	NTSVD	0.0449047	0.0442712	0.0405936
	Tikh(a)	0.0638937	0.0386419	
	Tikh(b)	<u>0.0401528</u>	0.0560726	
	Tikh(c)	0.0633967	0.0590594	
	Tikh(d)	-0.0009147	0.0539707	
	Tikh(e)	0.0476311	0.0583683	
Kimes.orchgrass	NTSVD	0.1082957	0.1058740	0.0783379
	Tikh(a)	0.0397185	0.0860485	
	Tikh(b)	<u>0.0753925</u>	0.1214918	
	Tikh(c)	0.26211583	0.4365220	
	Tikh(d)	-0.0018020	0.0383555	
	Tikh(e)	0.1137684	0.1707774	
Parabola.1994.asp-ifc2	NTSVD	0.0364620	0.0389198	0.0227972
	Tikh(a)	0.0447834	-0.0040831	
	Tikh(b)	<u>0.0262501</u>	0.0102457	
	Tikh(c)	0.0798633	-0.0874783	
	Tikh(d)	-0.0006110	-0.0401510	
	Tikh(e)	0.0375009	0.0547068	

chosen by a posteriori method addressed in section 2.6). The true white sky albedo (WSA) is calculated from well-posed situations using AMBRALS, i.e., full observation data. It deserves pointing out that the standard operational algorithm used in AMBRALS does not work for such severely ill-posed situations. If we regard $WSA > 1$ or $WSA < 0$ as failed inversion, it is clear that our proposed method works for all of the cases. It follows from the experiments that our new proposed method (Tikh(b)) works, for a single observation, and performs better than the NTSVD and the standard Tikhonov regularization with a priori choice of the regularization parameter (Tikh(a)).

3.3. Tests on Satellite Data: Insufficient Observation From Modis and TM

[25] In this test, we use atmospherically corrected moderate resolution imaging spectroradiometer (MODIS) 1B product acquired on a single day as an example of single observation BRDF at certain viewing direction. Each pixel has different view zenith angle and relative azimuth angle. The data MOD021KM.A2001135-150 with horizontal tile number (26) and vertical tile number (4) were measured covers Shunyi county of Beijing, China. The three parameters are retrieved by using this 1B product. Figure 1 plots the reflectance for band 1 of a certain day $DOY = 137$. In MODIS AMBRALS algorithm, when insufficient reflectances or a poorly representative sampling of high quality

Table 3. Comparison of Computational Values of the WSAs From the Data Sets in Table 1 for Single Observation and for Two Observations With the True WSAs Values (Multiangular Observations) for Nir Band

	Methods	Single Observation	Two Observations	True WSAs
Ranson_soy.827	NTSVD	0.4469763	0.4348320	0.3653728
	Tikh(a)	0.6359822	0.4195730	
	Tikh(b)	<u>0.3996775</u>	0.5439493	
	Tikh(c)	0.6310461	0.9247240	
	Tikh(d)	-0.0091045	-0.0098136	
	Tikh(e)	0.4741162	0.6277249	
Kimes.orchgrass	NTSVD	0.3890207	0.37216767	0.2963261
	Tikh(a)	0.2048903	0.2945934	
	Tikh(b)	<u>0.2708260</u>	0.4458619	
	Tikh(c)	0.9415755	1.8140732	
	Tikh(d)	-0.0064732	0.1927318	
	Tikh(e)	0.4086801	0.6015300	
Parabola.1994.asp-ifc2	NTSVD	0.5517209	0.5741842	0.4240376
	Tikh(a)	0.6776356	-0.0617838	
	Tikh(b)	<u>0.3972022</u>	0.2398577	
	Tikh(c)	1.2084479	-0.8953630	
	Tikh(d)	-0.0092437	-0.4071125	
	Tikh(e)	0.5674424	0.8185223	

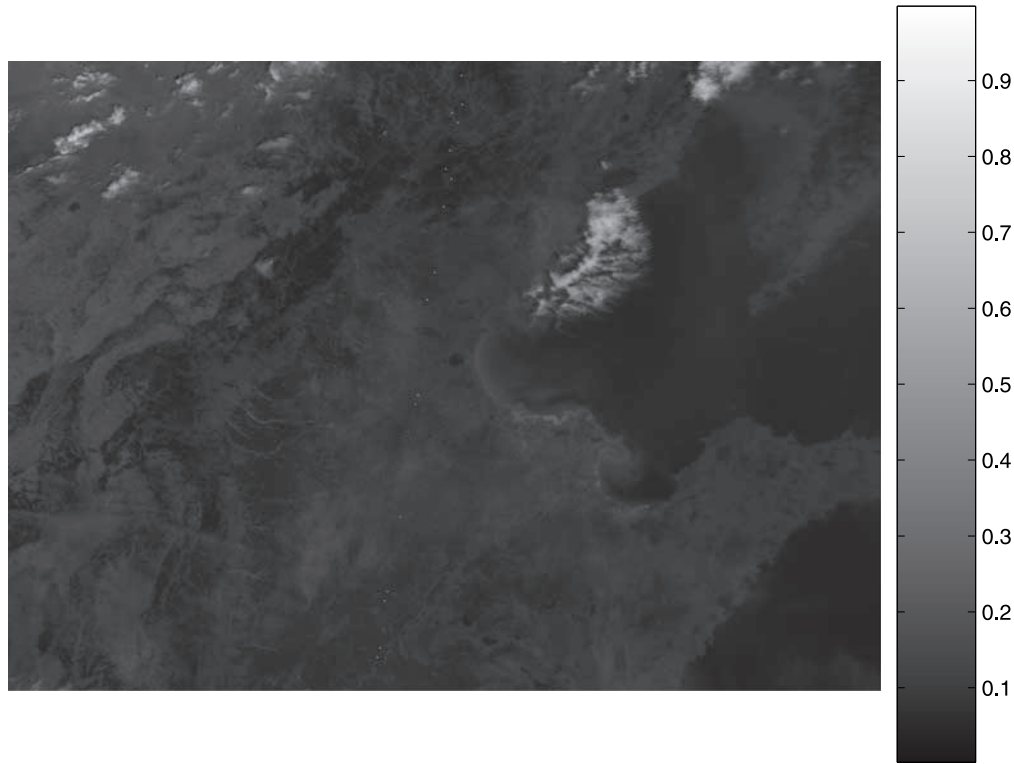


Figure 1. Reflectance for band 1 of MOD021KM.A2001137.

reflectances are available for a full inversion, a database of archetypal BRDF parameters is used to supplement the data and a magnitude inversion is performed [see *Verstraete et al.*, 1996; *Strahler et al.*, 1999]. We note that the standard MODIS AMBRALS algorithm cannot work for such an extreme case, even for MODIS magnitude inversion since it is hard to obtain seasonal data associated with a dynamic land cover in a particular site. But our method still works for such an extreme case because that smoothness constraint is implanted into the model already. Because of the limitations of the observation, there are black pixels with low energy in the retrieved albedo. Note that the albedo is the integration of the BRDF over all directions; therefore, there should be a similarity between the BRDF and the albedo. So, for low energy pixels of the albedo, we use a polynomial fitting from BRDF to obtain the corresponding albedo, and we plot the white-sky albedo (WSA) retrieved by Tikh(b) for band 1 of one observation (DOY = 137) in Figure 2. From Figure 2 we see that the albedo retrieved from insufficient observations can generate the general profile. We observe that most of the details are preserved though the results are not perfect. The results are similar to the one from NTSVD method developed by *Wang et al.* [2007]. Hence we conclude that both methods can be considered useful methods for retrieval of land surface parameters and for computing land surface albedos. Thus both algorithms can be considered as supplemental algorithms for the robust estimation of the land surface BRDF/albedos.

[26] We also test our algorithms to the Landsat Thematic Mapper (TM) data measured in Shunyi county of Beijing, China. The TM sensor is an advanced, multispectral scan-

ning, Earth resources instrument designed to achieve higher image resolution, sharper spectral separation, improved geometric fidelity, and greater radiometric accuracy and resolution. Figure 3 plots the reflectance for band 5 on 17 May 2001. The spatial resolution for the TM sensor on band 5 is 30 m. The white-sky albedo (WSA) retrieved by Tikh(b) for band 5 of one observation on 17 May 2001 is plotted in Figure 4. The retrieved results show that our algorithms work for satellite data with high spatial resolutions.

3.4. Discussion of the Numerical Results

[27] Experimental results on different data sets indicate that our proposed regularization method is feasible for ill-posed land surface parameter retrieval problems.

[28] We want to emphasize that our method can generate smoothing data for helping retrieval of parameters once sufficient observations are unavailable. As we have pointed out by *Wang et al.* [2007], we do not suggest discarding the useful history information (e.g., data that is not too old) and the multiangular data. Instead, we should fully employ such information if it is available. The key to why our algorithm outperforms previous algorithms is because that our algorithm is adaptive, accurate and very stable, which solves kernel-based BRDF model of any order, which may be a supplement for BRDF/albedo retrieval product.

[29] For the remote sensor MODIS, which can generate a product by using 16 d different observations data, this is not a strict restriction for MODIS, since it aims at global exploration. For other sensors, the period for their detection of the same area will be longer than 20 d or more. Therefore for vegetation in the growing season, the reflectance and



Figure 2. White-sky albedo retrieved by the proposed Tikhonov regularization method for band 1 of MOD021KM.A2001137.



Figure 3. Reflectance for band 5 of Landsat Thematic Mapper Data (TM) on 17 May 2001.



Figure 4. White-sky albedo retrieved by the proposed Tikhonov regularization method for band 5 of the Landsat Thematic Mapper Data (TM) on 17 May 2001.

albedos will change significantly. Hence robust algorithms to estimate BRDF and albedos in such cases are highly desired. Our algorithm is a proper choice, since it can generate retrieval results which quite approximate the true values of different vegetation type of land surfaces by capturing just one time of observation.

[30] Moreover, for some sensors with high spatial resolution, the quasi multiangular data are impossible to obtain. This is why there are not high resolution albedo products. But with our algorithm, we can achieve the results. This is urgently needed in real applications.

4. Concluding Remarks and Future Research

[31] A limited or insufficient number of observations is one of the most severe obstacles for a better estimation of BRDF, which leads to the ill-posed nature of model inversion. Therefore it is desirable to develop new techniques for the robust estimation of the BRDF model parameters due to scarcity of the number of observations. In this study, we thoroughly investigate the regularization methods, propose an a posteriori discrepancy method for choosing the regularization parameter and the creation of smoothness data to establish well-posedness.

[32] Our numerical simulations show that the regularization method proposed in this paper is suitable for solving ill-posed land surface parameter retrieval problems, and also applicable for inverse problems in other disciplinary sub-

jects in Earth surface parameter retrieval problems. Our algorithm can be considered as a supplement to BRDF/albedo algorithms.

[33] Since the regularization methods are based on the variational model, therefore, many optimization methods can be used to solve the problem. Interesting problems are how to construct efficient a priori information quantitatively from solution space of the problem to incorporate it into regularization model, and how to terminate iterative algorithms to yield optimality and regularity.

Appendix A: Morozov's Discrepancy Principle

[34] In this appendix, we recall the Morozov's discrepancy principle for the continuous abstract operator equation

$$y_n := y + n = Kx + n,$$

where K is an operator maps x to y and n is additive noise. The discrepancy $\|Kx - y_n\|$ refers to the norm of the deviation of the noisy observation to the true noise-free data. Here the norm $\|\cdot\|$ used above refers to the L_2 norm. Assume that the noise level (upper bound) for n is known as δ . Then Morozov's discrepancy principle requires solving the minimization problem [see Tikhonov and Arsenin, 1977; Xiao et al., 2003]

$$\|x\| \rightarrow \min$$

under the compact constraint

$$x \in S = \{x : \|Kx - y_n\| \leq \delta\}.$$

The Morozov's discrepancy principle is based on the viewpoint that the magnitude of the error should be in agreement with the accuracy of the assignment of the input data.

[35] Noting that S is closed and convex, the above minimization in Morozov's discrepancy principle has a unique vector of minimum norm on the boundary of the set S . We denote that unique vector by x_α . Therefore $\alpha = \alpha(\delta)$ by the criterion

$$\|Kx_\alpha - y_n\| = \delta$$

The assertion can be interpreted as that the discrepancy should be in agreement with the error in the input data.

[36] Denote by $\Psi(\alpha) = \|Kx_\alpha - y_n\|^2 - \delta^2$, it is easy to show that there is a unique value $\alpha = \alpha(\delta)$ of the regularization parameter satisfying $\Psi(\alpha) = 0$. The proof can be made by applying the following steps: (1) verify that $\Psi'(\alpha) > 0$, which indicates that $\Psi(\alpha)$ is increasing and continuous; and (2) show that $\Psi(\alpha) > 0$ as $\alpha \rightarrow \infty$ and $\Psi(\alpha) \leq 0$ as $\alpha \rightarrow 0$. The detail of the proof is left to the readers.

Appendix B: Computation of the Gradient of a Functional

[37] Let X and Y be Hilbert spaces, and $K: X \rightarrow Y$ be a bounded operator. Now we consider the operator equation

$$Kx = y, \quad x \in X, \quad y \in Y. \quad (\text{B1})$$

If the operator K does not have bounded inverse, the above operator equation would be ill-posed. Associated with the above operator equation, we define the Tikhonov functional as

$$J^\alpha(x) := \frac{1}{2} \|Kx - y\|_Y^2 + \frac{\alpha}{2} \|D^{1/2}x\|_X^2, \quad (\text{B2})$$

where $\alpha > 0$ is the regularization parameter and D is a positive (semi)definite operator. For any $h \in X$ and $\rho \in \mathbb{R}$, we have

$$\begin{aligned} J^\alpha(x + \rho h) &= \frac{1}{2} \left(\|Kx - y\|_Y^2 + \alpha \|D^{1/2}x\|_X^2 \right) \\ &\quad + \frac{\rho}{2} \left((Kx - y, Kh)_Y + (Kh, Kx - y)_Y \right) \\ &\quad + \alpha \left(D^{1/2}x, D^{1/2}h \right)_X + \alpha \left(D^{1/2}h, D^{1/2}x \right)_X \\ &\quad + \frac{\rho^2}{2} \left(\|Kh\|_Y^2 + \alpha \|D^{1/2}h\|_X^2 \right). \end{aligned}$$

Hence

$$\begin{aligned} \frac{d}{d\rho} J^\alpha(x + \rho h) \Big|_{\rho=0} &= (Kx - y, Kh)_Y + \alpha (Dx, h)_X \\ &= ((K^*K + \alpha D)x - K^*y, h)_X. \end{aligned}$$

which yields that the gradient is given by

$$\text{grad}[J^\alpha(x)] = (K^*K + \alpha D)x - K^*y.$$

[38] By the first-order necessary condition [see, e.g., Wang, 2007], the minimizer x_α should satisfy $\text{grad}[J^\alpha(x_\alpha)] = 0$, which gives $x_\alpha = (K^*K + \alpha D)^{-1}K^*y$.

Appendix C: Instructions on Implementing the Regularizing Algorithms

[39] The following are the procedures and subroutines of our regularization algorithms described above.

[40] *Creation of data D subroutine*: since the matrix D (D_1 - D_4) is in the diagonal form and is symmetric, therefore it is easy to make code.

[41] *A posteriori choice of the regularization parameter and solving the regularizing problem subroutine*: we list the procedure for computation as follows, so users can repeat the experiment easily.

[42] Algorithm C.1 (an a posteriori algorithm for solving the regularizing problem).

[43] *Step 1* Input \tilde{K} , \mathbf{y}_n , the error level $\delta > 0$, the initial guess value $\alpha_0 > 0$, k_{\max} and the stopping tolerance $\varepsilon > 0$, set $k = 0$;

[44] *Step 2* Solve equations (14)–(16);

[45] *Step 3* Compute $\Psi(\alpha_k)$, $\Psi'(\alpha_k)$ and $\Psi(\alpha_k)$;

[46] *Step 4* Update α_{k+1} by iterative formula (13);

[47] *Step 5* If $|\alpha_{k+1} - \alpha_k| \leq \varepsilon$ or $k = k_{\max}$, STOP; otherwise, set $k = k + 1$, GOTO Step 2.

[48] In our numerical tests, the parameters are $\alpha_0 = 0.001$, $\delta = 1.0 e-6$, $\varepsilon = 1.0 e-6$ and $k_{\max} = 100$. However, the step $k = k_{\max}$ is never activated.

[49] *Solving linear equations subroutine*: Solving the equations (14)–(16) can be easily completed by Cholesky decomposition method,

$$K^T K + \alpha D = G^T G,$$

then solving $G^T G \mathbf{x} = \mathbf{y}$ can be simply finished by solving

$$G^T \mathbf{u} = \mathbf{y}, \quad G \mathbf{x} = \mathbf{u}.$$

[50] **Acknowledgments.** We wish to express our sincere thanks for the very helpful comments from the anonymous referees and the editors which led to the improvement of this manuscript. We are also quite grateful to Hao Zhang who generously provided high resolution data for our numerical experiment. We want to give our special thanks to Qiyu Sun for his discussions and improvement on the paper. This work was supported by the National Natural Science Foundation of China under grant 10501051 and National "973" Key Basic Research Developments Program of China under grant 2007CB714400 and 2005CB422104.

References

- Atzberger, C. (2004), Object-based retrieval of biophysical canopy variables using artificial neural nets and radiative transfer models, *Remote Sens. Environ.*, 93, 53–67.
- Deering, D. W., T. F. Eck, and T. Grier (1992), Shinnery oak bidirectional reflectance properties and canopy model inversion, *IEEE Trans. Geosci. Remote Sens.*, 30(2), 339–348.
- Deering, D. W., E. M. Middleton, and T. F. Eck (1994), Reflectance anisotropy for a spruce-hemlock forest canopy, *Remote Sens. of Environ.*, 47, 242–260.

- Deering, D. W., S. P. Shmad, T. F. Eck, and B. P. Banerjee (1995), Temporal attributes of the bidirectional reflectance for three forest canopies, *Int. Geosci. Remote Sens. Symp. (IGARSS'95)*, 2, 1239–1241.
- Eck, T. F. and D. W. Deering (1992), Spectral bidirectional and hemispherical reflectance characteristics of selected sites in the streletskey steppe, in *Proceedings of the 1992 International Geoscience and Remote Sensing Symposium*, vol. 2, IEEE Geosci. Remote Sens. Soc., New Jersey, 1053–1055.
- Gao, F., A. H. Strahler, W. Lucht, Z. Xia, and X. Li (1998), Retrieving albedo in small sample size, *IEEE Int. Geosci. Remote Sens. Symp. Proc.*, 5, 2411–2413.
- Hu, B. X., W. Lucht, X. W. Li, and A. H. Strahler (1997), Validation of kernel-driven semiempirical models for the surface bidirectional reflectance distribution function of land surfaces, *Remote Sens. Environ.*, 62, 201–214.
- Kimes, D. S., W. W. Newcomb, and C. J. Tucker (1985), Directional reflectance factor distributions for cover types of northern Africa, *Remote Sens. Environ.*, 18, 1–19.
- Kimes, D. S., W. W. Newcomb, and R. F. Nelson (1986), Directional reflectance distributions of a hardwood and a pine forest canopy, *IEEE Trans. Geosci. Remote Sens.*, 24, 281–293.
- Li, X., J. Wang, and A. H. Strahler (1999), Apparent reciprocal failure in BRDF of structured surfaces, *Prog. Nat. Sci.*, 9, 747–750.
- Li, X., F. Gao, Q. Liu, J. D. Wang, and A. H. Strahler (2000), Validation of a new GO kernel and inversion of land surface albedo by kernel-driven model (1), *J. Remote Sens.*, 4, 1–7.
- Li, X., F. Gao, J. Wang, and A. H. Strahler (2001), A priori knowledge accumulation and its application to linear BRDF model inversion, *J. Geophys. Res.*, 106, 11,925–11,935.
- Pokrovsky, O., and J. L. Roujean (2002), Land surface albedo retrieval via kernel-based BRDF modeling. Part I: Statistical inversion method and model comparison, *Remote Sens. Environ.*, 84, 100–119.
- Pokrovsky, O. M., and J. L. Roujean (2003), Land surface albedo retrieval via kernel-based BRDF modeling. Part II: An optimal design scheme for the angular sampling, *Remote Sens. Environ.*, 84, 120–142.
- Pokrovsky, I. O., O. M. Pokrovsky, and J. L. Roujean (2003), Development of an operational procedure to estimate surface albedo from the SEVIRI/MSG observing system by using POLDER BRDF measurements. Part II: Comparison of several inversion techniques and uncertainty in albedo estimates, *Remote Sens. Environ.*, 87(2–3), 215–242.
- Privette, J. L., T. F. Eck, and D. W. Deering (1997), Estimating spectral albedo and nadir reflectance through inversion of simple bidirectional reflectance distribution models with AVHRR/MODIS-like data, *J. Geophys. Res.*, 102, 29,529–29,542.
- Roujean, J. L., M. Leroy, and P. Y. Deschamps (1992), A bidirectional reflectance model of the Earth's surface for the correction of remote sensing data, *J. Geophys. Res.*, 97, 20,455–20,468.
- Strahler, A. H., X. W. Li, S. Liang, J.-P. Muller, M. J. Barnsley, and P. Lewis (1994), *MODIS BRDF/Albedo Product: Algorithm Technical Basis Document*, NASA EOS-MODIS Doc., vol. 2.1, 55 pp.
- Strahler, A. H., W. Lucht, C. B. Schaaf, T. Tsang, F. Gao, X. Li, J. P. Muller, P. Lewis, and M. J. Barnsley (1999), *MODIS BRDF/Albedo Product: Algorithm Theoretical Basis Document*, NASA EOS-MODIS Doc., V5.0, 53 pp. (URL: <http://modarch.gsfc.nasa.gov/MODIS/LAND/#albedo-BRDF>)
- Tarantola, A. (1987), *Inverse Problems Theory: Methods for Data Fitting and Model Parameter Estimation*, 613 pp., Elsevier, New York.
- Tikhonov, A. N., and V. Y. Arsenin (1977), *Solutions of Ill-Posed Problems*, John Wiley, Hoboken, N. J.
- Tikhonov, A. N., A. V. Goncharsky, V. V. Stepanov, and A. G. Yagola (1995), *Numerical Methods for the Solution of Ill-Posed Problems*, Springer, New York.
- Verstraete, M. M., B. Pinty, and R. B. Myneny (1996), Potential and limitations of information extraction on the terrestrial biosphere from satellite remote sensing, *Remote Sens. Environ.*, 58, 201–214.
- Wang, Y. F. (2007), *Computational Methods for Inverse Problems and Their Applications*, Higher Educ. Press, Beijing.
- Wang, Y. F., and T. Y. Xiao (2001), Fast realization algorithms for determining regularization parameters in linear inverse problems, *Inverse Probl.*, 17, 281–291.
- Wang, Y. F., and Y. X. Yuan (2003), A trust region algorithm for solving distributed parameter identification problem, *J. Comput. Math.*, 21(6), 759–772.
- Wang, Y. F., X. W. Li, S. Q. Ma, H. Yang, Z. Nashed, and Y. N. Guan (2005), BRDF model inversion of multiangular remote sensing: Ill-posedness and interior point solution method, in *Proc. 9th Int. Symp. Physical Measurements and Signature in Remote Sens. (ISPMRSR)*, vol. XXXVI, edited by S. Liang et al., pp. 328–330.
- Wang, F., F. Fan, X. Feng, J. Yan, and N. Guan (2006a), Regularized inversion method for retrieval of aerosol particle size distribution function in $W^{1,2}$ space, *Appl. Opt.*, 45, 7456–7467.
- Wang, Y. F., Z. Nashed, and X. W. Li (2006b), Non-statistical regularized methods for land surface parameter retrieval, in *Proc. Int. Conf. Tikhonov Contemp. Math.*, Section No. 4, pp. 215–216, Moscow.
- Wang, Y. F., X. W. Li, Z. Nashed, F. Zhao, H. Yang, Y. N. Guan, and H. Zhang (2007), Regularized kernel-based BRDF model inversion method for ill-posed land surface parameter retrieval, *Remote Sens. Environ.*, 111, 36–50.
- Wanner, W., X. Li, and A. H. Strahler (1995), On the derivation of kernels for kernel-driven models of bidirectional reflectance, *J. Geophys. Res.*, 100, 21,077–21,090.
- Xiao, T. Y., S. G. Yu, and Y. F. Wang (2003), *Numerical Methods for the Solution of Inverse Problems*, Science Press, Beijing.

X. Li, State Key Laboratory of Remote Sensing Science and Research Center for Remote Sensing and GIS, Beijing Normal University, 19 Xijiekouwai Street Beijing, 100875, China.

Y. Wang and C. Yang, Institute of Geology and Geophysics, Chinese Academy of Sciences, No. 19, Beitucheng Xilu, Chaoyang District, P.O. Box 9825, Beijing 100029, China. (yfwang@mail.iggcas.ac.cn)